

Observations on edge GAM-turbulence interactions in ASDEX Upgrade

G.D.Conway¹, F.Palermo¹, I.Novikau¹, P.Simon², P.Hennequin³, and the ASDEX Upgrade Team

¹Max-Planck Institut für Plasmaphysik, 85748 Garching, Germany

²National Institute for Fusion Science, Oroshi-cho, Toki-shi, Gifu 509-5292, Japan

³Laboratoire de Physique des Plasmas, Ecole Polytechnique, 91128 Palaiseau, France

1. Introduction

The interaction of Geodesic Acoustic Modes (GAMs), Zonal Flows and small-scale turbulence is an important topic in magnetic confinement studies. In recent years much progress has been made in the area of measurement, interpretation and numerical simulation. Previously on ASDEX Upgrade tokamak (AUG) microwave Doppler reflectometry (DR) has been used to investigate the temporal and spatial behaviour of coherent edge GAMs [1]. Here, new results are presented on the non-linear interaction of GAMs with both the background incoherent flow u_{\perp} fluctuations and the ambient density n_e turbulence.

GAMs (few kHz, $m = n = 0$, coherent $E \times B$ flow oscillations) generally exist in the tokamak edge between the separatrix and the n_e pedestal. For weak pedestals they may extend significantly further in, depending on Landau damping. Fig. 1(a) shows a perpendicular velocity $u_{\perp} = 2\pi f_D/k_{\perp}$ profile, plus DR shift f_D and amp. $A_D \propto \tilde{n}_e$ spectra for a low density, NBI heated, lower-single-null (LSN) L-mode. The GAM p.t.p. can reach $> 30\%$ of u_{\perp} at the tokamak outer mid-plane [1a].

2. Zonal structure

The GAM radial structure is zonal with either a continuum frequency ($f_{GAM} \propto c_s$) or one or more eigenmodes ($f_{GAM} = \text{constant}$), as in fig. 1 (shaded region), or even multi-mode, as in fig. 5 for a circular, limiter L-mode. What determines the zonal structure is a topic of current investigation. The GAM amplitude A_{GAM} profile is asymmetric, generally peaking towards the outer zonal boundary. In fig. 1(c) the maxima is in the n_e gradient region where the turbulence drive, i.e. pressure gradient $\nabla_r P$, is large but the flow shear $\nabla_r u_{\perp}$ is weak. The zonal width is usually a few cm, consistent with meso-scale wavelengths $\lambda_r \sim \sqrt{a\rho_i} \sim 3 - 4$ cm, where a and ρ_i are plasma minor radius and ion Larmor radius.

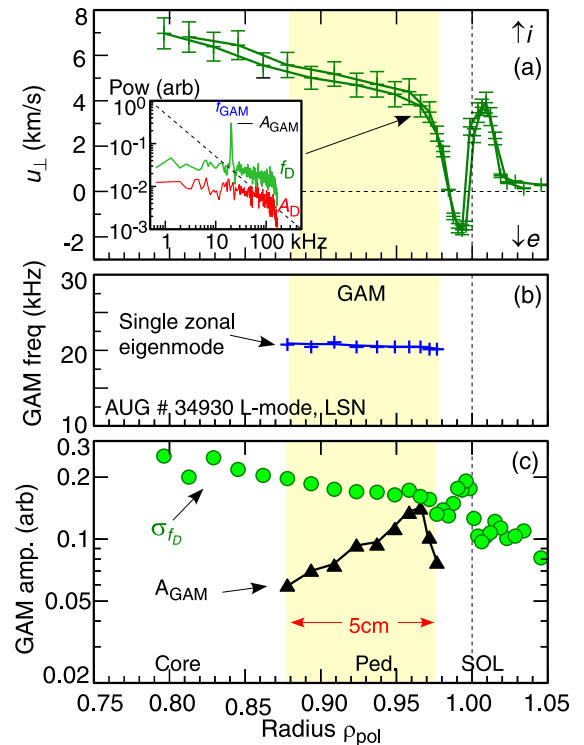


Fig. 1: (a) u_{\perp} , (b) f_{GAM} , (c) A_{GAM} and flow σ_{f_D} profiles for LSN L-mode #34930.

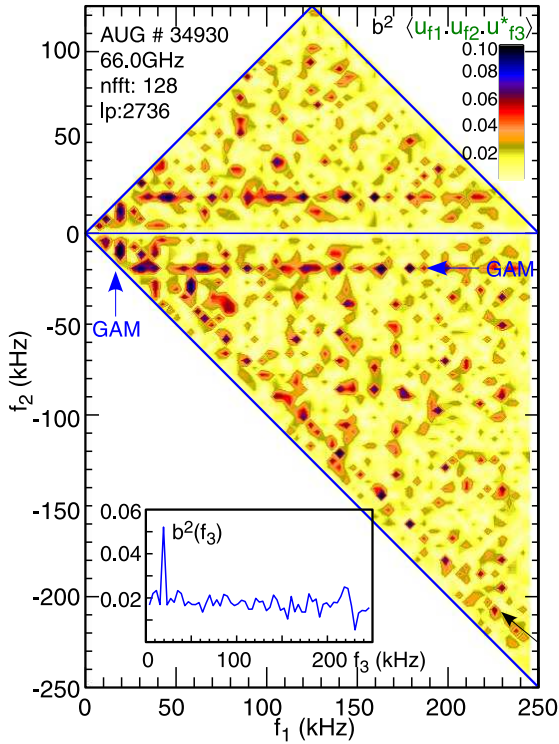


Fig. 2: (a) Flow \tilde{u}_\perp auto-bicoherence b^2 , (b) $b^2(f_3)$ spectrum at GAM maxima, #34930.

suggests the GAM is driven at the location of maximum turbulence and non-linear coupling, and then spreads radially inward and outward towards the zonal boundaries, cf. the geometrical optics description [6].

Towards the core, as the GAM weakens, the f_D flow spectra flattens and the flow fluctuation RMS level σ_{f_D} rises, fig. 1(c), coinciding with a significant increase in the total (full-band) \bar{b}^2 coupling - open triangles in fig. 3(a) - although the n_e turbulence falls.

4. Energy transfer

While the bispectra shows GAM-turb. coupling, it does not give the energy transfer direction of the coupling. One technique, based theory-wise on the high freq. n_e turbulence being modulated by the GAM, involves high-pass filtering the A_D (turb.) signal then extracting the envelope using a Hilbert transform $Env(A_D) = |A_D + iH(A_D)|$ [2,4]. Fig. 4 shows segments of band-pass filtered f_D ($f_{GAM} \pm 1$ kHz) flow and $Env(A_D)$ [30 – 300] kHz signals which are correlated (cf. dashed lines) confirming the HF n_e fluctuations are modulated at the GAM frequency

3. Non-linear drive

Bispectral & biphasic analysis has been used widely to study the non-linear drive of the GAM via 3-wave coupling, cf. [2-5]. The squared bicoherence is given by: $b^2(f_1, f_2) = |B(f_1, f_2)|^2 / \langle |X(f_1)X(f_2)|^2 \rangle \langle |X(f_3)|^2 \rangle$, with $B(f_1, f_2) = \langle X(f_1)X(f_2)X^*(f_3) \rangle$ the bispectrum, $f_3 = f_1 \pm f_2$, and Fourier mode $X(f_n)$. Fig. 2 shows the flow auto-bicoherence at the GAM radial peak in #34930. The coupling of the broad-band fluctuations to the GAM appears as ridges at f_{GAM} in $f_1, \pm f_2$ & f_3 , cf. $b^2(f_3)$ spectra. The total bicoherence $\bar{b}^2 = \sum_{f_1} \sum_{f_2} b^2(f_1, f_2) / N$, i.e. b^2 integrated over f_1 and f_2 , is an indicator of the total non-linear activity. In fig. 3(a) the radial profiles of \bar{b}^2 and $b^2(f_3) = \sum_{f_3=f_1+f_2} b^2(f_1, f_2)$ at $f_3 = f_{GAM}$ (GAM coupling) show maxima aligning with the GAM intensity A_{GAM} peak, fig. 1(c). This

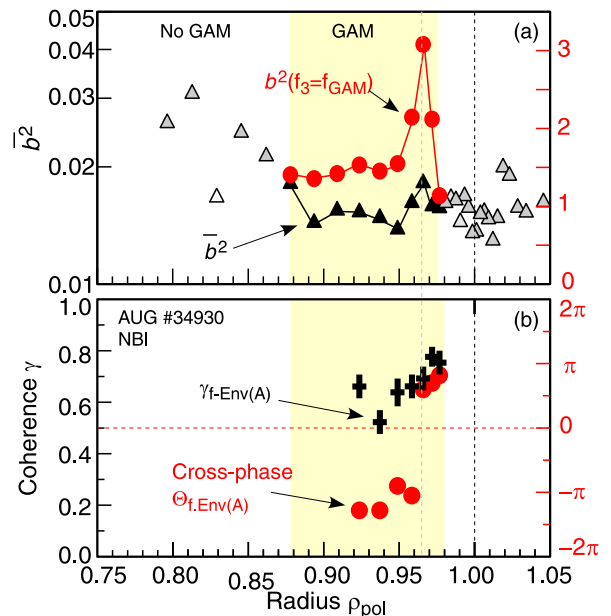


Fig. 3: (a) \bar{b}^2 and $b^2(f_{GAM})$ and (b) flow-turb. coherence γ & cross-phase Θ profiles, #34930.

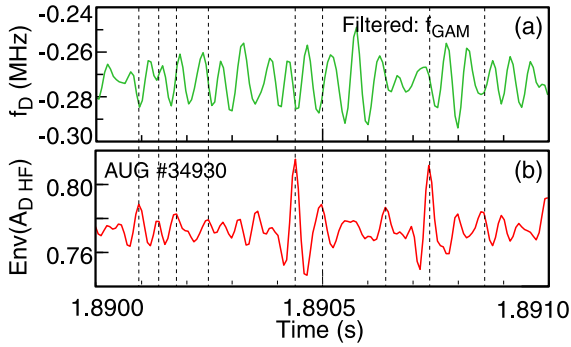


Fig. 4: Section of filtered f_D and $Env(A_D)$ signals at GAM peak, LSN L-mode #34930.

with radial propagation velocities of a few hundred ms^{-1} [7] - implying the GAM and turbulence decorrelate as the GAM propagates.

5. GAM frequency modulation

At its spatial maxima the GAM is highly coherent with a spectral width Δf_{fwhm} (indicative of the GAM lifetime) of only a few hundred Hz. However, at the zonal boundaries the GAM spectral peak broadens to several kHz as it weakens and decays faster, as shown by the Δf profile (down-triangles) in fig. 5(c) for the circular, limiter L-mode #34953.

In this discharge there is a radial region where two continuum GAMs appear to overlap and, as shown by the amplitude profiles, switch dominance. Nevertheless, even for single eigenmode or continuum GAMs, the GAM spectral peak will exhibit a fine frequency splitting - as shown in fig. 6(a) for LSN L-mode #29725. The effect is more clearly seen in the corresponding band-pass filtered f_D auto-correlation of fig. 6(b) by double decay times τ_x , with $\rho \propto \exp(-|\tau/\tau_x|)$. Where a single GAM is dominant, fig. 5(a), the initial short decay $\tau_S^{-1} \sim f_{GAM}$, is set by the GAM frequency, while the later long decay is inverse to the spectral width, $0.5/\tau_L \sim \Delta f_{fwhm}$. With multiple GAM peaks there is strong inter-modulation and $1/\tau_S \ll f_{GAM}$. This behaviour is indicative of a low frequency modulation (FM) of the GAM.

6. GAM amplitude modulation

The GAM amplitude A_{GAM} also displays a low frequency (typically between 40 – 400 Hz) intermittency or ‘breathing’ with up to 50% modulation, roughly correlated, but phase-shifted to a corresponding modulation of f_{GAM} [1a].

and thus non-linear coupled. From the relative phase the GAM generally leads the turbulence, but the phase delay shifts and reverses with time and radial position. Fig. 3(b) shows the profile of coherence γ and cross-phase Θ between f_D and $Env(A_D)$ at f_{GAM} . As with $b^2(f_3)$, the γ also peaks at the GAM outer edge while Θ progressively varies (and reverses) across the GAM peak - consistent

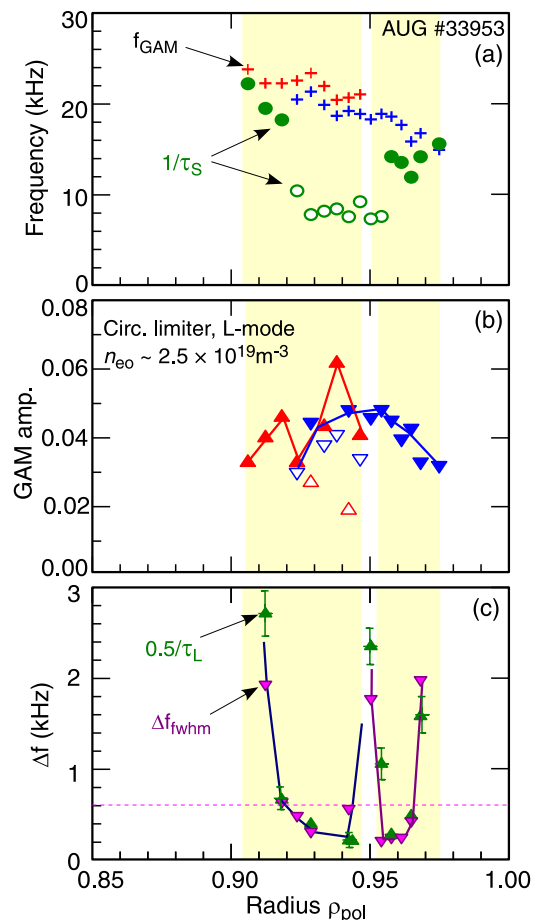


Fig. 5: (a) f_{GAM} & $1/\tau_S$, (b) A_{GAM} and (c) GAM width Δf_{fwhm} & $0.5/\tau_L$ profiles for circular, limiter, L-mode #34953.

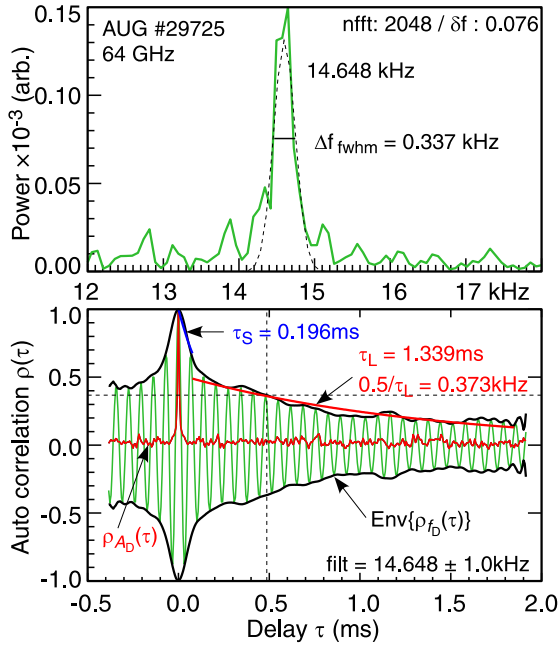


Fig. 6: (a) Flow f_D power spectra and (b) auto-correlation of GAM band-pass filtered f_D (gn) at GAM peak, L-mode #29725.

Towards the zonal edges the GAM decays faster - suggesting the energy spreads radially away from the GAM maxima as the GAM propagates. While the GAM tends to lead the n_e turbulence (i.e. GAM modifies turb.) their relative phase varies and reverses in time. Taken with the spectral behaviour this suggests the energy moves back and forth between the GAM and the turbulence both temporally and spectrally. The low frequency modulation of the GAM and the HF turbulence is suggestive of either a LF zonal flow oscillation, or close frequency beating between two radially overlapping GAMs.

References

- [1] G.D.Conway *et al.*, Plasma Phys. Control. Fusion [a] **47**, 1165 (2005), [b] **50**, 055009, [c] **50**, 085005 (2008)
- [2] Y.Nagashima *et al.*, Plasma Phys. Control. Fusion **48**, A377 (2006)
- [3] Y.Hamada *et al.*, Nucl. Fusion **50**, 025001 (2010)
- [4] A.D.Lui *et al.*, Plasma Phys. Control. Fusion **52**, 085004 (2010)
- [5] A.V.Melnikov *et al.*, Nucl. Fusion **57**, 115001 (2017)
- [6] F.Palermo *et al.*, Proc. 45th EPS Conf. ECA **42A**, P1.1100 (2018)
- [7] P.Simon, Ph.D. Thesis, Uni. Stuttgart (2017)

The GAM temporal modulation is more clearly seen in the f_D (flow) spectrogram of fig. 7(a) for #29725. Below, are time traces of integrated power over the GAM peak ($P_{f_D(\text{GAM})}$: 12 – 18 kHz) and the high frequency HF band $P_{f_D(\text{HF})} > 18$ kHz, as well as the corresponding HF n_e turbulence $P_{A_D(\text{HF})}$. The adjacent power spectra show the GAM and n_e turb. primarily LF modulated, around 47 Hz with other peaks at 124 Hz and 260 Hz. Generally, $P_{f_D(\text{GAM})}$ and $P_{f_D(\text{HF})}$ are out of phase [1a], i.e. energy moves within the flow spectrum, while $P_{f_D(\text{GAM})}$ and $P_{A_D(\text{HF})}$ are in-phase at 47 Hz, but otherwise phase-shifted.

7. Conclusions

Bispectral analysis shows the non-linear coupling of the broad-band flow u_{\perp} and n_e turbulence to the GAM at a narrow radial location, corresponding to a strong ∇P and weak ∇u_{\perp} region.

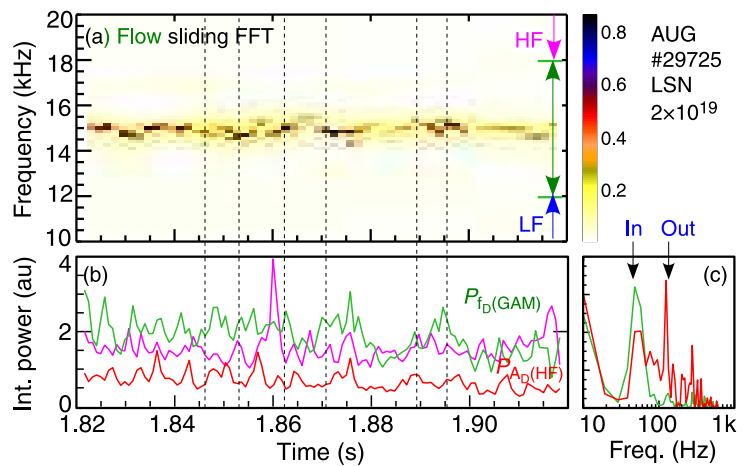


Fig. 7: (a) f_D spectrogram, (b) integrated power traces over GAM and HF ranges with (c) spectra, at GAM radial maxima for LSN, L-mode #29725